

Capacity-constrained demand response in smart grids using deep reinforcement learning

Shafagh Abband Pashaki^a, Sepehr Maleki^a, Amir Badiee^a

^a*Lincoln AI Lab, University of Lincoln, Lincoln, United Kingdom*

Abstract

This paper presents a capacity-constrained incentive-based demand response approach for residential smart grids. It aims to maintain electricity grid capacity limits and prevent congestion by financially incentivising end users to reduce or shift their energy consumption. The proposed framework adopts a hierarchical architecture in which a service provider adjusts hourly incentive rates based on wholesale electricity prices and aggregated residential load. The financial interests of both the service provider and end users are explicitly considered. A deep reinforcement learning approach is employed to learn optimal real-time incentive rates under explicit capacity constraints. Heterogeneous user preferences are modelled through appliance-level home energy management systems and dissatisfaction costs. Using real-world residential electricity consumption and price data from three households, simulation results show that the proposed approach effectively reduces peak demand and smooths the aggregated load profile. This leads to an approximately 22.82% reduction in the peak-to-average ratio compared to the no-demand-response case.

Keywords: Smart Grid, Incentive-Based Demand Response, Home Energy Management System, Deep Reinforcement Learning

1. Introduction

Demand Response (DR) is a mechanism used by suppliers to manage real-time fluctuations in electricity networks. In such schemes, suppliers offer

. *Email addresses:* spashaki@lincoln.ac.uk (Shafagh Abband Pashaki), smaleki@lincoln.ac.uk (Sepehr Maleki), abadiee@lincoln.ac.uk (Amir Badiee)

incentives to consumers to manage their power consumption during peak periods [1]. This requires enabling consumers to lower their energy usage by reducing the load, shifting their consumption over time, or generating and storing energy at certain times [2]. In modern smart grids, advanced Information and Communication Technology (ICT) and Advanced Metering Infrastructure (AMI) enable bidirectional communication between power suppliers and consumers. As a result, DR has emerged as an important mechanism for improving the reliability and sustainability of power systems [3, 4]. Despite its potential benefits, DR plays a limited role in most countries due to lack of trust, concerns about risk, and the complexity of participation [5]. As a result, electricity supply and demand are balanced by ensuring that generation, reserves and network capacity are sufficient to meet demand [6]. A well-designed DR scheme can improve the balance between electricity supply and demand, enhance grid efficiency, and increase system flexibility, particularly in modern smart grids. Traditionally, the balance between supply and demand in the electricity network was managed by building enough power plants and infrastructure. In contrast, DR programmes help reduce supply costs by reducing the need for expensive new power plants or infrastructure that would only be used during peak load situations [7].

DR methods are broadly classified into two main categories, namely price-based demand response (PBDR) and incentive-based demand response (IBDR) [8]. In PBDR, consumers adjust their electricity consumption in response to time-varying electricity prices [9]. IBDR programmes, on the other hand, provide fixed or time-varying incentives to customers to change or reduce their energy consumption during peak periods [10, 11]. IBDR programmes are more dispatchable and less risky with respect to delivered flexibility compared to PBDR programmes, as power suppliers can more directly aim for and achieve a specific target level of load reduction via the incentive mechanism [12]. Besides, it has been recognised that IBDR programmes are generally viewed as reward-based programmes in practice and exhibit more enduring and stable participant engagement, leading to more sustained benefits for consumers [13]. Approximately 93% of peak load reductions in the United States are achieved through IBDR programmes [14, 15].

DR programmes can be implemented in residential, commercial, and industrial establishments in a very similar manner [16]. The residential sector, which accounts for more than 40% of the total electricity demand, significantly impacts the electricity network and contributes to 30% of greenhouse

gas emissions [17]. A DR scheme can flexibly manage residential loads under varying circumstances and can also incorporate strategies such as load profile management, strategy-driven conservation measures, and adjustments to consumer segments and market participation levels [18]. Residential users participate and respond to DR programmes with varying levels of engagement across households. Financial and environmental benefits are commonly associated with residential participation in DR, with financial incentives often attracting greater attention. Nevertheless, concerns related to privacy, autonomy, and the perceived clarity of benefits may affect user trust and engagement [5]. Transparent mechanisms, clear communication, and the involvement of trusted local actors have been identified as important elements for fostering participation in residential DR programmes. More broadly, residential DR is more likely to be adopted when the resulting economic savings outweigh perceived discomfort or loss of convenience, as many consumers exhibit limited willingness to compromise comfort for lower electricity costs [6].

Challenges. Despite the extensive development of DR programmes, designing effective real-time IBDR for residential smart grids remains challenging. In practice, residential DR must simultaneously (i) respect explicit grid capacity limits to prevent congestion, (ii) adapt to highly dynamic and uncertain electricity prices and consumption patterns, and (iii) account for heterogeneous end-user (EU) comfort preferences at the appliance level. Traditional approaches often rely on static or day-ahead formulations and simplified aggregate demand models, which limit their ability to respond to fast-changing operating conditions and to accurately represent household-level flexibility. As a result, many existing DR schemes struggle to deliver reliable peak reduction while maintaining sustained residential participation and acceptable EU comfort.

Existing solutions and limitations. Existing solutions to IBDR largely fall into two categories. On the one hand, model-based approaches such as mathematical optimisation, game-theoretic, and elasticity-based methods have been widely studied. While these methods provide analytical insight, they require strong modelling assumptions, accurate parameter estimation, and often lack scalability or real-time applicability in realistic residential settings. On the other hand, recent reinforcement learning (RL)-based approaches have demonstrated promising performance in learning adaptive incentive-setting or scheduling strategies from data. However, in many existing RL-based studies, EU response is modelled at an aggregated level,

appliance-level flexibility is treated separately from incentive design, or grid capacity constraints are handled implicitly or under simplified assumptions. Consequently, there remains a gap between data-driven incentive learning and practical, capacity-aware residential DR with detailed device-level modelling.

Our contributions. To address these challenges, this paper proposes a capacity-constrained reinforcement learning-based demand response (CCRL-DR) framework for residential smart grids. The proposed approach explicitly integrates grid capacity limits into the RL state and reward formulation, enabling real-time, capacity-aware incentive design. A hierarchical architecture is considered, in which a service provider (SP) learns optimal hourly incentive rates based on wholesale electricity prices and aggregated residential demand. Heterogeneous EU preferences are modelled through appliance-level home energy management systems (HEMSs) and dissatisfaction costs. By combining deep RL with device-level response modelling and real-world load and price data, the proposed framework achieves effective peak shaving and load smoothing without inducing rebound peaks. Comparative simulations against an elasticity-based load reduction (EBLR) benchmark demonstrate that CCRL-DR delivers superior peak-to-average ratio (PAR) reduction while maintaining EU comfort and economic viability for both the SP and the EUs.

2. Literature Review

Until now, a great deal of work has been devoted to the design of IBDR mechanisms for smart grids. These studies mainly rely on model-based formulations, including coupon/credit schemes, game-theoretic designs, and optimisation-based scheduling. The study in [19] presents a coupon-based DR strategic bidding model for a load-serving entity under wind uncertainty. The problem is formulated as a bi-level stochastic optimisation and reformulated as a mixed-integer linear programming (MILP) problem to maximise the load-serving entity’s profit. In a similar work, Li et al. [20] develop a dynamic coupon-based IBDR programme for distributed energy systems with multiple load aggregators. Coupons incentivise EUs to reduce peak-period demand and minimise operating cost, while a fairness function ensures equitable incentive distribution across aggregators. Erdinc et al. [21] propose a credits-based incentive mechanism for EUs to reduce critical load demand and maintain the balance between supply and demand during peak periods.

Ambient temperature uncertainty is incorporated within a stochastic day-ahead framework. The studies [22, 23] formulate grid operator-centric IBDR as a three-level hierarchy comprising a grid operator (GO), multiple SPs, and their EUs. The GO first announces an incentive to SPs, who then run EU-facing programmes and offer incentives to enrolled EUs to agree on specific demand-reduction amounts. In view of this hierarchical decision-making structure, a Stackelberg game is adopted to capture the interactions among these different participants. In [24], an improved IBDR is presented in which the elasticity is modelled as a function of price, time (hour), and EU type. The proposed IBDR can participate in both day-ahead and intra-day markets with time-varying incentive rates. Similarly, the work in [25] estimates incentive-based elasticity at the appliance level and shows that calculating elasticity at this level is more informative for operational decision-making than feeder-level value aggregated elasticity.

Beyond market design and incentive formulation, a number of studies have focused on incorporating uncertainty, risk management, and system-level operational constraints into IBDR programmes. In [26], a risk management scheme for the SP is presented to address uncertainties in the day-ahead market and mitigate financial losses. This is achieved by combining an IBDR programme for EUs with distributed generation and energy storage systems. In a similar work, [27] proposes a multi-objective short-term IBDR scheduling model to manage market price risk and load uncertainty. In this framework, DR scheduling is performed simultaneously with the dispatch of generation and storage units while accounting for grid-imposed capacity obligations (e.g., capacity charges/penalties) and the resulting optimisation problem is solved using the non-dominated sorting genetic algorithm II (NSGA-II). In [28], a contract-based IBDR scheme between an aggregator and a single EU is developed to induce individual rationality and asymptotic incentive compatibility. Under this scheme, the EU self-reports its baseline and reduction capacity. In more advanced classical studies, linear and non-linear modelling for the IBDR programmes is implemented in four different power markets [29]. It revealed that the DR programmes can shift part of the electricity demand and save energy, while may lead to different demand pattern with different responsive load behavioural model. In [30], a nonlinear IBDR is used in unit commitment problem by considering the nonlinear behaviours of residential EUs.

However, most of the above-mentioned efforts on IBDR rely on traditional

model-based methods, including stochastic programming, game-theoretic formulations, and MILP. These approaches typically require explicit system modelling and the identification of parameters that are dependent on EU characteristics, which can be difficult to obtain in practice. Moreover, model-based formulations often rely on simplifying assumptions that may limit their applicability in real-world residential settings. Although some studies incorporate uncertainty or capacity-related terms, these aspects are generally handled within offline or model-based frameworks. In addition, several existing works focus on a single EU or assume homogeneous users, thereby overlooking the impact of multiple EUs with heterogeneous characteristics. Furthermore, a large portion of the literature investigates DR in the context of day-ahead markets, while real-time operation is considered under more restrictive assumptions.

In recent years, RL has been increasingly adopted as an AI-based approach for sequential decision-making, in which an agent learns a policy through interaction with an environment to maximise cumulative reward [31]. In the context of smart energy management, RL-based methods have been applied to a variety of decision-making problems, including energy scheduling and incentive design [32]. For example, in [33], a model-assisted batch RL is applied to building climate control under dynamic pricing. The sequential decision-making problem is formulated as a Markov Decision Process (MDP), and a control policy is learned via fitted Q-iteration. In addition, Mahapatra et al. [34] develop an advanced neural fitted Q-learning approach to manage home appliances. The approach aims to reduce peak-period power load, promote energy conservation, and reduce the carbon footprint of residential dwellings. In one application [1], a single-agent Q-learning-based HEMS approach is proposed. Human preferences are considered by directly integrating user feedback into the control logic using fuzzy reasoning to shape the reward, enabling appliance scheduling through peak-to-off-peak load shifting. In [35], a Deep Reinforcement Learning (DRL) approach is proposed for home energy management, to optimise Photovoltaic (PV) self-consumption, focusing on domestic heating and hot-water systems. In a related study [36], a data-driven DRL-based HEMS optimisation framework is developed to handle uncertain household parameters and high-dimensional, time-coupled decision-making. The methodology integrates a BiGRU-NN prediction model for forecasting PV output and electricity prices with a Soft Actor-Critic (SOC) agent to derive control policies and optimise scheduling decisions.

In another approach to home energy management [37], this method successfully schedules diverse load types, including non-shiftable, power-shiftable, time-shiftable appliances, and EVs, ensuring a balance between operational efficiency and EU comfort. Similarly, the authors of [38] present a decentralised multi-agent learning-based residential DR framework to better align household consumption with variable wind availability, thereby improving renewable integration in smart homes.

While the above studies mainly focus on household-level energy management, a separate line of research applies RL to IBDR, where decision-making is performed at the system or SP level. In one study, a single-agent RL framework is used to compute optimal incentive rates for heterogeneous EUs, where the trade-off between EU incentive income and dissatisfaction is jointly balanced with the SP's objective [39]. Building on this formulation, [40] extends the same incentive-based RL framework by incorporating PV generation, while [41] further augments the model by including historical incentive information in the decision-making process. In [11], a decentralised Multi-Agent Reinforcement Learning (MARL) approach is applied to an IBDR programme. A uniform incentive is provided to all residential EUs to reduce energy consumption while maintaining grid capacity constraints and preventing congestion. The incentive mechanism encourages heterogeneous EUs to participate while preserving their privacy. A novel disjunctively constrained knapsack problem optimization is incorporated to curtail or shift household appliance consumption based on the selected demand reduction. In [42], the authors propose a model-free framework for multi-household appliance scheduling formulated as a noncooperative stochastic game. Distributed DRL is applied to search for the Nash equilibrium consumption while preserving household privacy. In [43], a cooperative multi-household MARL approach is used to schedule controllable appliances to minimize total energy costs while enforcing global physical constraints. Both approaches emphasize the ability to scale with the number of EUs and operate in real time.

Overall, these studies demonstrate that RL can learn sequential decision policies through interaction with uncertain environments and balance cost objectives with EU comfort considerations. In the closest RL-based works on residential IBDR, consumer response is often modelled at an aggregated EU level. Appliance-level modelling is typically studied in HEMS settings without tight coupling to incentive-setting mechanisms. In addition, although some RL formulations incorporate uncertainty or capacity-related terms,

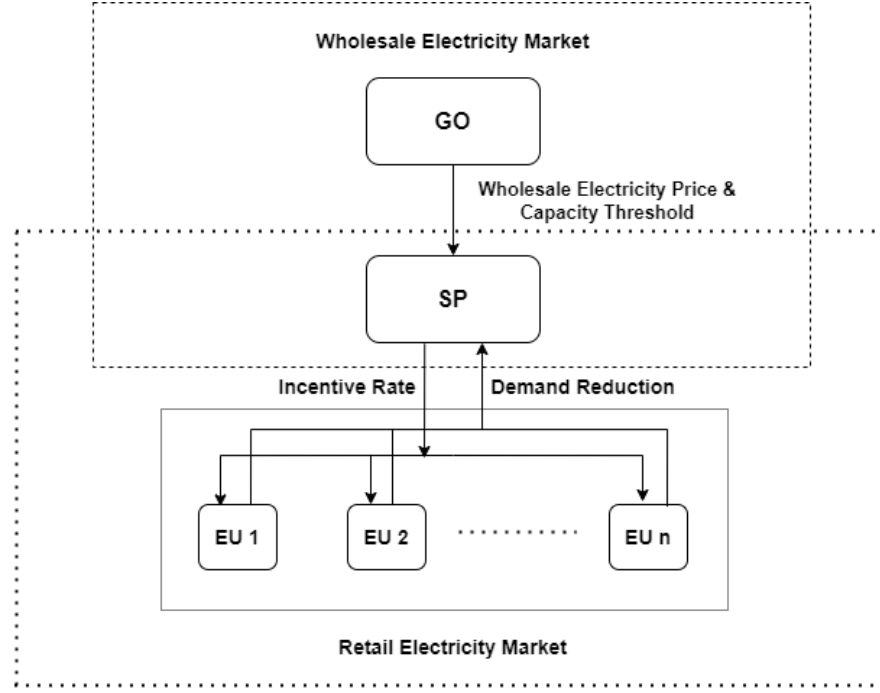


Figure 1: Hierarchical electricity market model.

these aspects are typically handled implicitly or under simplified settings, particularly with respect to scalable and real-time operation under physical grid constraints.

3. Demand response model

In this section, we describe the system model and the interaction between the GO, SP, and residential EUs as shown in Fig. 1. The GO interacts with the wholesale market and announces both the hourly wholesale price and a capacity limit for the aggregated residential load. The SP purchases energy at the wholesale price and manages the demand of the participating EUs at the retail level. The SP communicates hourly financial incentive rates to the EUs, while the resulting demand adjustments are aggregated at the SP level. The aggregated load is constrained to remain below or close to the capacity limit, while EU discomfort is modelled through explicit dissatisfaction costs.

3.1. Service provider model

The SP is the main aggregator and decision maker in the proposed IBDR programme. For each hour h , the SP observes the aggregated demand of the residential EUs and how close it is to the contractual capacity limit. Taking into account the wholesale price announced by the GO, the SP then sets hourly financial incentives to encourage EUs to reduce or shift part of their flexible demand when the aggregated demand approaches this limit. From the SP's perspective, these demand reductions provide demand-side flexibility by lowering the amount of energy that must be purchased from the wholesale market; therefore, the SP's performance is evaluated using the profit function in Eq. (1).

$$\max \sum_{h=1}^H \sum_{n=1}^N (p_h \Delta E_{n,h} - \lambda_{n,h} \Delta E_{n,h}), \quad (1)$$

$$\lambda_{\min} \leq \lambda_{n,h} \leq \lambda_{\max}, \quad \forall n, h, \quad (2)$$

where $n = 1, \dots, N$ denotes the index of EUs and $h = 1, \dots, H$ is the hourly time index. The term p_h is the wholesale price at hour h , $\Delta E_{n,h}$ is the effective demand reduction of EU n at hour h , and $\lambda_{n,h}$ is the incentive rate offered to that EU. The product $p_h \Delta E_{n,h}$ represents the saving in wholesale energy cost due to the reduction, whereas $\lambda_{n,h} \Delta E_{n,h}$ corresponds to the incentive payment [39, 40]. The bounds λ_{\min} and λ_{\max} specify an allowed range for the incentive rates, which can be interpreted as contractual or regulatory limits, and keep the offered incentives within a reasonable and practical level for both the SP and the EUs [19, 22].

3.2. End user model

In the DR programme, each residential EU is assumed to be equipped with a HEMS, where applicable, that adjusts part of its flexible energy demand in response to financial incentives proposed by the SP. By participating in the programme, the EU can obtain a monetary reward when reducing its demand, at the cost of modifying its preferred consumption pattern. In each decision period, the HEMS determines the amount of flexible demand to curtail or shift in time. Accordingly, the objective of each EU can be written as

$$\max \sum_{h=1}^H \left[\rho \lambda_{n,h} \Delta E_{n,h} - (1 - \rho) C_{n,h}^{\text{dis}} \right]. \quad (3)$$

The first term in Eq.(3) represents the EU's financial benefit from participating in the DR programme, while the second term corresponds to the dissatisfaction cost. Here, $\rho \in [0, 1]$ is a weighting factor that reflects the trade-off between financial benefit and comfort. Larger values of ρ correspond to EUs that are more responsive to financial incentives, whereas smaller values indicate EUs that place more emphasis on maintaining their comfort level. Similar to [44, 11], $C_{n,h}^{\text{dis}}$ denotes the dissatisfaction cost of the n -th EU in hour h .

In each household n , the appliance set \mathcal{D}_n is divided into three subsets, time-shiftable appliances $\mathcal{D}_n^{\text{TS}}$, power-controllable appliances $\mathcal{D}_n^{\text{PC}}$ (e.g., air conditioner), and non-shiftable appliances $\mathcal{D}_n^{\text{NS}}$, which do not participate in the DR programme and therefore remain unchanged, such that $\mathcal{D}_n = \mathcal{D}_n^{\text{TS}} \cup \mathcal{D}_n^{\text{PC}} \cup \mathcal{D}_n^{\text{NS}}$. In this work, time-shiftable appliances are classified as either interruptible or non-interruptible. Interruptible time-shiftable appliances $\mathcal{D}_n^{\text{TS,I}}$ (e.g., EV charging) can be paused and resumed in later hours, subject to meeting the daily energy requirement and the completion deadline. In contrast, non-interruptible time-shiftable appliances $\mathcal{D}_n^{\text{TS,NI}}$ (e.g., washing machine, dishwasher, and dryer) must operate as a continuous block once started. The total flexible energy reduction of EU n in hour h is then obtained by aggregating the contributions of all flexible appliances,

$$\Delta E_{n,h} = \sum_{a \in \mathcal{D}_n^{\text{PC}}} \Delta E_{n,a,h}^{\text{PC}} + \sum_{a \in \mathcal{D}_n^{\text{TS,I}}} \Delta E_{n,a,h}^{\text{TS,I}} + \sum_{a \in \mathcal{D}_n^{\text{TS,NI}}} \Delta E_{n,a,h}^{\text{TS,NI}}, \quad (4)$$

where $\Delta E_{n,a,h}^{\text{PC}}$ denotes the energy demand reduction obtained by curtailing the consumption of power-controllable appliance a at hour h . The term $\Delta E_{n,a,h}^{\text{TS,I}}$ represents the flexible energy reduction resulting from temporarily reducing or postponing the operation of interruptible time-shiftable appliance a (e.g., shifting EV charging to later hours). Finally, $\Delta E_{n,a,h}^{\text{TS,NI}}$ captures the energy demand reduction obtained by rescheduling the indivisible operating block of non-interruptible time-shiftable appliance a away from high-load hours. Whenever part of a time-shiftable appliance's energy demand is moved from a peak hour to lower-load hours (or hours below the capacity limit), the energy removed from that peak hour is counted in the corresponding $\Delta E_{n,a,h}^{\text{TS,I}}$

or $\Delta E_{n,a,h}^{\text{TS,NI}}$, while the same amount reappears in later hours as additional actual energy consumption. In this way, $\Delta E_{n,h}$ summarises both the curtailment of energy demand from PC appliances and the removal/relocation of TS loads from congested hours [44, 11]. Accordingly, non-shiftable appliances $\mathcal{D}_n^{\text{NS}}$ do not contribute to $\Delta E_{n,h}$.

To capture heterogeneous comfort preferences, we assign each controllable appliance $a \in \mathcal{D}_n^{\text{PC}} \cup \mathcal{D}_n^{\text{TS}}$ of EU n an appliance-specific dissatisfaction coefficient $\beta_{n,a} > 0$, which quantifies the residents' discomfort due to power curtailment or time shifting. In practice, $\beta_{n,a}$ is a user-defined parameter that residents can update in their HEMS according to their preferences [11]. For PC appliances, we use a finite set of discrete curtailment levels [45]. The curtailment level of appliance a in household n and hour h is represented by an integer $q_{n,a,h} \in \{0, 1, \dots, m_a\}$, where m_a is the number of available levels for that appliance. In practice, the actual energy reduction is implemented as a fraction of $E_{n,a,h}$, and the same fraction is used inside the dissatisfaction cost. The disutility from curtailing a PC appliance is then written as

$$C_{n,a,h}^{\text{PC}} = \beta_{n,a} \left(\frac{q_{n,a,h}}{m_a} E_{n,a,h} \right)^2, \quad (5)$$

and the corresponding energy reduction at level $q_{n,a,h}$ is

$$\Delta E_{n,a,h}^{\text{PC}}(q_{n,a,h}) = \frac{q_{n,a,h}}{m_a} E_{n,a,h}. \quad (6)$$

For a given incentive rate $\lambda_{n,h}$, the HEMS selects the curtailment level that maximises the net utility of appliance a in hour h ,

$$q_{n,a,h}^* \in \arg \max_{q \in \{0, 1, \dots, m_a\}} [\lambda_{n,h} \Delta E_{n,a,h}^{\text{PC}}(q) - C_{n,a,h}^{\text{PC}}(q)], \quad (7)$$

and we write $\Delta E_{n,a,h}^{\text{PC}}$ in Eq.(4) as a shorthand for $\Delta E_{n,a,h}^{\text{PC}}(q_{n,a,h}^*)$. This discrete best-response formulation is consistent with the search over a finite set of curtailment rates implemented in the numerical model.

For TS appliances (both interruptible and non-interruptible), the dissatisfaction is assumed to increase with the delay between the requested and the actual starting time of the appliance. Let $\Delta T_{n,a,h}$ denote the accumulated delay (in hours or time steps) when appliance a of EU n is actually operated in hour h . The associated dissatisfaction cost is modelled as

$$C_{n,a,h}^{\text{TS}} = \beta_{n,a} \Delta T_{n,a,h}^2, \quad (8)$$

so that longer waiting times result in higher discomfort.

In the implementation, each non-interruptible TS appliance is represented as a continuous operating block of fixed length. When an incentive is offered and shifting is allowed, the HEMS searches over a finite set of feasible alternative starting times that respect the appliance-specific completion deadline, while also ensuring that the capacity limit is not violated. Among these candidates, the block is moved to an hour where the aggregated load is relatively low, so that the original operation during peak hours is replaced by operation in less congested periods. Accordingly, $\Delta E_{n,a,h}^{\text{TS,NI}}$ in Eq.(4) represents the energy removed from the original peak hours.

For interruptible TS appliances, the daily energy requirement is distributed over a given charging window. The HEMS adjusts the hourly charging profile in response to the incentive signal by favouring hours with lower load and sufficient remaining capacity, while ensuring that the total required energy is delivered before the end of the window. Similarly, $\Delta E_{n,a,h}^{\text{TS,I}}$ in Eq.(4) captures temporary reductions or postponements of appliance operation during high-load hours.

We denote the total dissatisfaction cost of EU n in hour h by $C_{n,h}^{\text{dis}}$:

$$C_{n,h}^{\text{dis}} = \sum_{a \in \mathcal{D}_n^{\text{PC}}} C_{n,a,h}^{\text{PC}} + \sum_{a \in \mathcal{D}_n^{\text{TS}}} C_{n,a,h}^{\text{TS}}, \quad (9)$$

which aggregates the discomfort caused by both power curtailment and time shifting across all controllable appliances of EU n . Substituting Eqs.(4) and (9) into (3) expresses the EU objective directly in terms of appliance-level demand reductions and their dissatisfaction costs.

3.3. Objective function

Considering the profits of both the SP and the EUs, the final objective function is presented as follows:

$$\max \sum_{h=1}^H \left\{ \sum_{n=1}^N \left[\underbrace{(p_h - \lambda_{n,h}) \Delta E_{n,h}}_{\text{SP's profit}} + \underbrace{\rho \lambda_{n,h} \Delta E_{n,h} - (1 - \rho) C_{n,h}^{\text{dis}}}_{\text{EU's profit}} \right] + \Phi_h \right\}. \quad (10)$$

In the numerical implementation, we augment the hourly reward r_h with a shaping term Φ_h to encourage practically desirable behaviours while keeping

the economic structure of Eq. (10) unchanged. Specifically, Φ_h comprises four components; (i) a constant bonus of +5 when no reduction is required and no incentives are issued, (ii) a penalty of $-5 \sum_{n=1}^N \lambda_{n,h}$ when no reduction is required but incentives are still sent, (iii) a penalty proportional to the unmet reduction, $-15 R_h^{\text{miss}}$, which is doubled if $\sum_{n=1}^N \lambda_{n,h} = 0$ despite a positive required reduction, and (iv) an over-reduction penalty of $-0.5 R_h^{\text{over}}$ to discourage unnecessary curtailment beyond the required level. Here, R_h^{miss} and R_h^{over} denote the missing and excess reductions at hour h , respectively.

4. Incentive optimisation

In the proposed IBDR scheme, the SP is modelled as the RL agent. In this section, we model the decision-making problem as a finite-horizon MDP, define the state, action, and reward, and employ a Double Deep Q-Network (DDQN) algorithm to learn an incentive rate policy.

4.1. Markov decision process for incentive-based demand response

MDP has been widely adopted to study RL-based decision-making problems. A MDP provides a classical framework for sequential decision making, where the actions taken by the agent influence not only the immediate reward, but also the subsequent states and hence future rewards. It is characterised by the Markov property, namely that the state transitions depend only on the current state and current action, and are independent of all previous states and actions. In the MDP model considered here, the key components are a discrete hour index $h \in \{1, \dots, H\}$, a state $s_h \in \mathcal{S}$, an action $a_h \in \mathcal{A}$ and a reward $r_h = R(s_h, a_h)$. One episode of this MDP thus constitutes the finite sequence $(s_1, a_1, r_1), (s_2, a_2, r_2), \dots, (s_H, a_H, r_H)$, where H denotes the final hour in the decision horizon.

In line with the above MDP formulation, Fig. 2 illustrates the RL-based decision-making structure adopted in this work, where the SP serves as the agent and the participating residential EUUs are considered the environment. At each hour, the SP announces a vector of incentive rates as the action. In response, the residential EUUs adjust their electricity consumption. The resulting aggregated load, electricity price, and required demand reduction with respect to the capacity limit define the system state and the per-hour reward r_h , as given in Eq. (11). The reward r_h corresponds to the hourly contribution of the global objective defined in Eq. (10).

$$r_h = \sum_{n=1}^N \left[(p_h - \lambda_{n,h}) \Delta E_{n,h} + \rho \lambda_{n,h} \Delta E_{n,h} - (1 - \rho) C_{n,h}^{\text{dis}} \right] + \Phi_h. \quad (11)$$

Taking the long-term returns into account, the SP must consider not only the current reward but also future rewards. The cumulative discounted reward from hour h is defined as

$$G_h = \sum_{k=h}^H \gamma^{k-h} r_k, \quad (12)$$

where $\gamma \in [0, 1]$ is the discount factor that controls the relative importance of future versus present rewards. Under a given policy π , the action–value function of taking action a_h in state s_h is defined as

$$Q^\pi(s_h, a_h) = \mathbb{E}_\pi[G_h \mid s_h, a_h]. \quad (13)$$

The optimal value is then $Q^*(s_h, a_h) = \max_\pi Q^\pi(s_h, a_h)$. An optimal policy can then be derived by selecting, in each state, the action with the highest action–value. In the following subsection, we describe how $Q^*(s_h, a_h)$ is approximated using a DDQN algorithm.

4.2. Double Deep Q -Network

In problems with a relatively high-dimensional and continuous state space, a tabular representation of the action–value function $Q(s, a)$ is not practical. Instead, we approximate $Q(s, a)$ by a deep neural network $Q(s, a; \theta)$ with parameters θ , which takes the current state s_h as input and outputs one Q-value per discrete incentive action [46]. Each discrete action corresponds to a pre-defined vector of incentive rates. To improve learning stability and mitigate the overestimation bias of standard deep Q -networks (DQN), we adopt a DDQN architecture. The DDQN algorithm employs two neural networks, denoted by Q and Q^- , which share the same network architecture but have different parameter sets. The parameters θ of the policy network Q are used to select the action corresponding to the maximum Q-value, while the parameters θ^- of the target network Q^- are used to evaluate the Q-value of the selected action [47, 48].

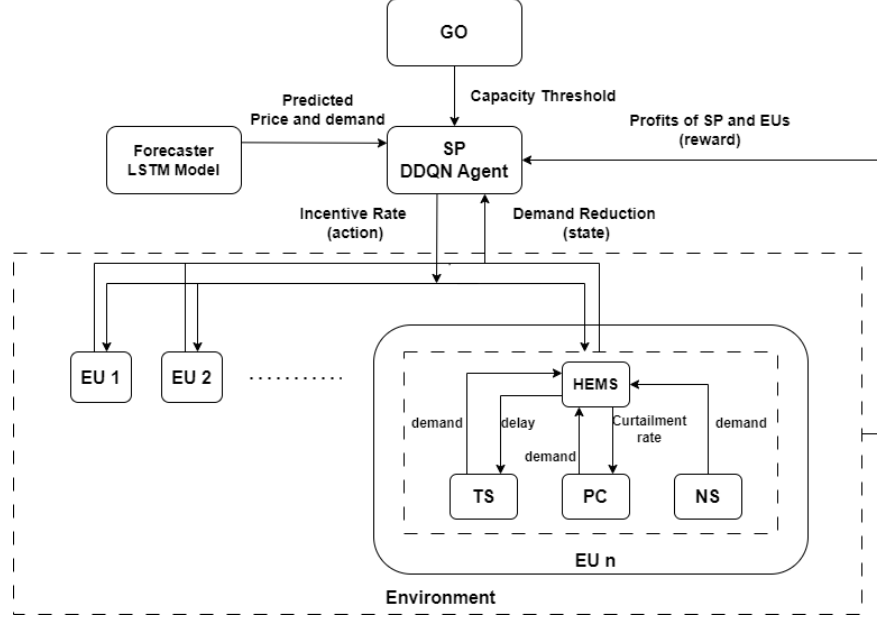


Figure 2: Schematic of RL to find the optimal incentive rates.

During training, transitions of the form $(s_h, a_h, r_h, s_{h+1}, \text{done}_h)$, where $\text{done}_h \in \{0, 1\}$ indicates whether the episode has terminated at hour h , are stored in a replay buffer \mathcal{B} . Mini-batches are sampled uniformly from \mathcal{B} to update the policy network [49]. For a sampled transition indexed by j , the DDQN target is computed as

$$y_j = r_j + \gamma(1 - \text{done}_j) Q\left(s'_j, \arg \max_{a'} Q(s'_j, a'; \theta); \theta^-\right), \quad (14)$$

where s'_j denotes the next state and γ is the discount factor introduced in Eq.(12). The parameters θ of the policy network are then updated by minimising a squared-error (Huber) loss between y_j and the current estimate $Q(s_j, a_j; \theta)$ over the mini-batch. The target-network parameters θ^- are updated more slowly using a soft update rule,

$$\theta^- \leftarrow \tau \theta + (1 - \tau) \theta^-, \quad (15)$$

with a small $\tau \in (0, 1)$ specified in the configuration.

4.3. Real-time algorithm with LSTM forecasts and DDQN

To implement the CCRL-DR framework in practice, we combine the LSTM-based forecasting models with the DDQN scheme described in the previous

subsections. Algorithm 1 summarises the resulting real-time IBDR procedure. Each episode corresponds to a single day and consists of H hourly decision steps. At the beginning of each episode, time-dependent input variables such as the day of the week, hour of the day, and seasonal indicators are constructed for all hours $h = 1, \dots, H$ and fed into the pre-trained LSTM models. These models then generate predictions of the wholesale electricity price F_{uPrice} and the aggregated residential load F_{uLoad} by rolling their one-step-ahead forecasts over the whole day. The forecasted values for each hour are later incorporated into the RL state, providing the agent with a forward-looking view of the expected operating conditions.

In the DDQN control loop, the environment is initialised with the forecasted price and load trajectories. At each hour h , the SP agent observes the current state s_h (including forecasts, current load, and capacity information) and selects an incentive rate vector $a_h = \{\lambda_{n,h}\}$ using an ε -greedy policy derived from the policy network. The environment applies these incentive rates, and the EUs adjust their appliance-level consumption according to the HEMS models. The resulting demand reductions and updated load profile yield the next state s_{h+1} and the immediate reward r_h , based on the per-hour contribution of the global objective in Eq. (10). The transition $(s_h, a_h, r_h, s_{h+1}, \text{done})$ is stored in the replay buffer, and when the buffer has enough samples, mini-batches are sampled to update the policy network parameters by minimising the DDQN loss with target values defined in Eq. (14). The target network parameters are softly updated towards the policy parameters using the rule in Eq. (15), and the exploration rate ε is gradually decayed according to a predefined schedule.

Table 1: Algorithm for real-time IBDR with LSTM and DDQN

Inputs: policy network $Q(s, a; \theta)$, target network $Q(s, a; \theta^-)$, replay buffer \mathcal{B} , weighting factor ρ , DDQN hyperparameters $(\gamma, \varepsilon, \tau, \alpha)$, incentive rate bounds $\lambda_{\min}, \lambda_{\max}$.
1: for episode $e = 1, \dots, N_{\text{ep}}$ do
2: % LSTM-based price forecasting
3: for hour $h = 1, \dots, H$ do
4: $\text{DofWeek}[h] \leftarrow \text{updateDayOfWeek}(h); \text{HofDay}[h] \leftarrow \text{updateHourOfDay}(h); \text{MofYear}[h] \leftarrow \text{updateMonthOfYear}(h);$
5: $\text{IsWeekend}[h] \leftarrow \text{updateWeekendFlag}(h); \text{IsHoliday}[h] \leftarrow \text{updateHolidayFlag}(h)$
6: $\text{PrSeq}[h] \leftarrow \text{updateHistoricalPriceSequence}()$
7: $\text{FuPrice}[h] \leftarrow \text{PriceLSTM}(\text{DofWeek}[h], \text{HofDay}[h], \text{MofYear}[h],$
8: $\text{IsWeekend}[h], \text{IsHoliday}[h], \text{PrSeq}[h])$
9: end for
10: % LSTM-based load forecasting
11: for hour $h = 1, \dots, H$ do
12: $\text{LoSeq}[h] \leftarrow \text{updateHistoricalLoadSequence}()$
13: $\text{FuLoad}[h] \leftarrow \text{LoadLSTM}(\text{DofWeek}[h], \text{HofDay}[h], \text{MofYear}[h],$
14: $\text{IsWeekend}[h], \text{IsHoliday}[h], \text{LoSeq}[h])$
15: end for
16: % DDQN-based incentive learning
17: $s_1 \leftarrow \text{Environment.reset}(\text{FuPrice}, \text{FuLoad})$ and obtain initial state s_1 .
18: for decision step (hour) $h = 1, \dots, H$ do
19: Using an ε -greedy policy derived from the policy network, select $a_h = \{\lambda_{n,h}\}_{n=1}^N$, where $\lambda_{n,h} \in [\lambda_{\min}, \lambda_{\max}]$.
20: Environment applies $\lambda_{n,h}$, computes demand reductions and the total reward r_h , and returns next state s_{h+1} and termination flag $\text{done} \in \{0, 1\}$.
21: Store $(s_h, a_h, r_h, s_{h+1}, \text{done})$ in replay buffer \mathcal{B} .
22: if \mathcal{B} has enough samples and an update step is due then
23: Sample a mini-batch $(s_j, a_j, r_j, s'_j, \text{done}_j)$ from \mathcal{B} .
24: Select the next greedy action using the policy network:
25: $a^* \leftarrow \arg \max_{a'} Q(s'_j, a'; \theta)$.
26: Compute the DDQN target: $y_j = r_j + \gamma(1 -$
27: $\text{done}_j) Q(s'_j, a^*; \theta^-)$.
28: Update θ to minimise the loss: $L = \mathbb{E}[(y_j - Q(s_j, a_j; \theta))^2]$.
29: Soft-update the target network: $\theta^- \leftarrow \tau\theta + (1 - \tau)\theta^-$.
30: end if
31: Update ε according to the exploration decay.
32: if done then break.
33: end for
34: end for

5. Experimental analysis

In this section, we present the results obtained by applying our proposed approach using real-world data. We evaluated the precision of our forecasting models and the effectiveness of our CCRL-DR scheme.

5.1. Price and load forecasting

We adopt LSTM-based DNN models for both price and load forecasting and use their one-step-ahead predictions as external inputs to the proposed IBDR scheme. Following the preprocessing methodology in [11], we utilized publicly available residential load datasets from Dataport [50] and extracted hourly load data for three randomly selected residential EUs located in Austin, Texas, USA, over the period from 1 April 2018 to 30 September 2018. This interval covers the months with the highest residential electricity consumption and peak load patterns, providing a suitable context for evaluating DR strategies. The testing period for the DR experiments was set to 1–31 July 2018, and is kept distinct from the training set. In parallel, wholesale price data for the same period were collected from the ERCOT market via EnergyOnline [51], with training and testing splits aligned with those of the load data.

To generate the required forecasts, we developed two separate LSTM-based DNN models. One model predicts the hourly wholesale electricity price, while three identical models predict the load of each individual EU, and the aggregated residential load is obtained by summing these forecasts. The two models share the same overall architecture but are trained independently on their respective historical time series. Adequate selection of input variables is critical for reliable performance [39, 40]. For both targets, the input feature vector at each time step includes time-related variables (month of year, day of week, hour of day, and binary indicators for holidays and weekends) together with recent historical values of the quantity to be forecast. Short-term dynamics are represented by several lagged observations from the previous hours, whereas longer-term patterns are captured by including values from the same hour on previous days. The full set of input features for the price and load forecasting models is summarised in Table 2.

Forecasting with the proposed LSTM-based models follows a standard supervised learning pipeline [52]. Each training sample consists of an input sequence constructed from the features in Table 2 and the corresponding

Table 2: Inputs to the LSTM-based forecasting models

Inputs for price forecasting		Inputs for load forecasting	
Index	Description	Index	Description
1	Month of year (1–12)	1	Month of year (1–12)
2	Day of week (1–7)	2	Day of week (1–7)
3	Hour of day (1–24)	3	Hour of day (1–24)
4	Is holiday (0 or 1)	4	Is holiday (0 or 1)
5	Is weekend (0 or 1)	5	Is weekend (0 or 1)
6	Price of hour $h - 1$	6	Load of hour $h - 1$
7	Price of hour $h - 2$	7	Load of hour $h - 2$
8	Price of hour $h - 3$	8	Load of hour $h - 3$
9	Price of hour $h - 24$	9	Load of hour $h - 24$
10	Price of hour $h - 25$	10	Load of hour $h - 25$
11	Price of hour $h - 26$	11	Load of hour $h - 26$
12	Price of hour $h - 48$	12	Load of hour $h - 48$
13	Price of hour $h - 49$	13	Load of hour $h - 49$
14	Price of hour $h - 50$	14	Load of hour $h - 50$

target value (future price or load at hour h). The network parameters are updated by backpropagation through time, using the mean squared error (MSE) between predicted and true values as the loss function and the Adam optimiser for gradient-based updates [53]. The main hyper-parameters, including the number of LSTM layers, hidden units, dropout rate, window size and forecast horizon, are reported in Table 3. To generate the required forecasts, we developed two separate LSTM-based DNN models. One model predicts the hourly wholesale electricity price, while three identical models predict the load of each individual EU, and the aggregated residential load is obtained by summing these forecasts. After training, the LSTM-based DNNs are kept fixed and, at each hour, map the most recent input sequence to one-step-ahead forecasts of the wholesale price and aggregated residential load [54].

Figs. 3 and 4 compare the predicted and actual electricity prices and load demands during the final week of the testing period (23–29 July 2018). In these plots, the actual values are depicted by solid red lines, while the forecasted values are shown by blue dashed lines. The corresponding forecast errors, quantified in terms of Mean Absolute Error (MAE) and Mean Abso-

Table 3: Hyper-parameters of the LSTM-based forecasting models

Hyper-parameter	Value
Number of LSTM layers	2
Hidden units	64
Dropout	0.2
Window size	24
Forecast horizon	1
Optimiser	Adam
Loss function	MSE

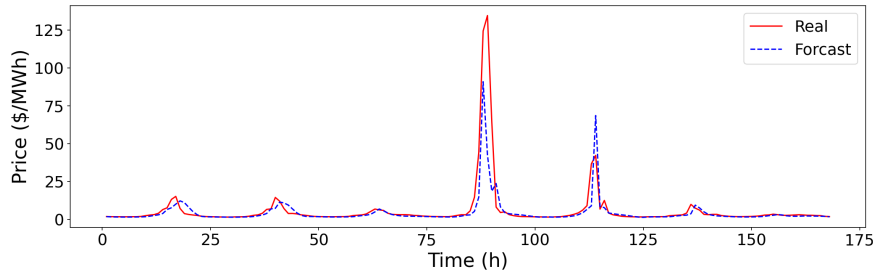
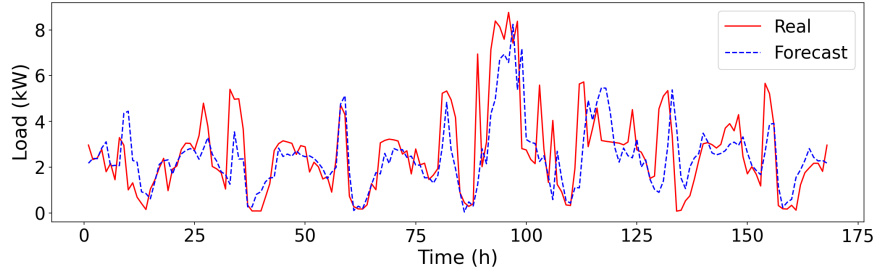
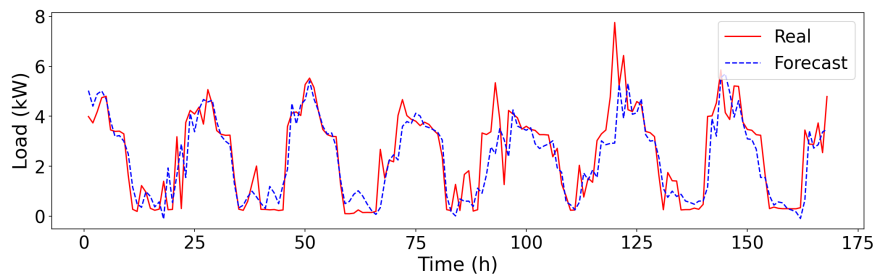


Figure 3: Wholesale price forecasting for July 23–29, 2018.

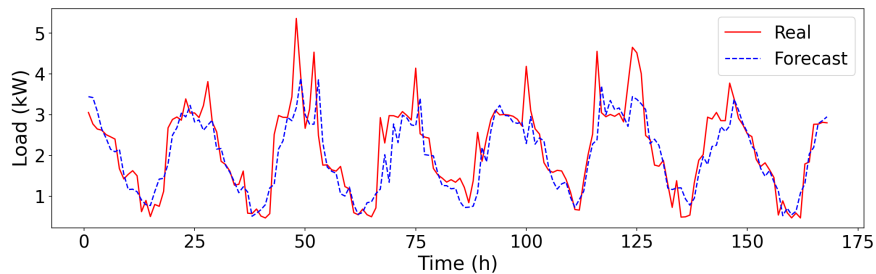
lute Percentage Error (MAPE), are summarised in Table 4. The relatively low MAE and MAPE values indicate good forecasting accuracy. In addition, the adopted LSTM architecture closely tracks the main daily and weekly patterns in both prices and loads, making it suitable for use within the proposed CCRL-DR framework.



(a) End User 1



(b) End User 2



(c) End User 3

Figure 4: Load forecasting of the three end users for July 23–29, 2018.

Table 4: Accuracy results of the forecasting model

	MAE	MAPE
Wholesale price forecasting model	1.87	0.53
Load forecasting model of EU1	0.90	0.93
Load forecasting model of EU2	0.72	0.78
Load forecasting model of EU3	0.41	0.24

5.2. Evaluation

In this part, we describe how we applied our RL-based algorithm to manage electricity consumption using the forecasts generated by our price and load models. Specifically, we utilized the forecasted data for July 27, 2018, to assess the algorithm’s effectiveness. The objective was to keep total electricity consumption within a predetermined capacity threshold while considering financial benefits for both the SP and EUs.

5.2.1. Simulation Setup

For evaluating the performance of the proposed RL-based DR algorithm, we conduct simulations using a simplified scenario consisting of a single SP and three residential EUs. Each EU corresponds to a real household in the 2018 data set (house IDs 661, 3039, and 8565). In all simulations, the hourly load and price trajectories fed to the RL environment are the forecasted values obtained from our forecasting models. The aggregate capacity threshold for the three EUs is set to 75% (approximately 7 kW) of the average daily peak of their total demand and is kept fixed throughout training and testing.

In the simulations, we use the DDQN-based framework to determine hourly incentive rates for each EU. The incentive bounds are set to $\lambda_{\min} = 0$ and $\lambda_{\max} = 0.95 p_h$, such that the incentives are directly tied to the current market price and never exceed 95% of p_h . To model the trade-off between incentive income and dissatisfaction cost on the EU side, we use a weighting factor ρ in the EU-level reward; in all simulations we set $\rho = 0.9$ and assume it is identical for all EUs. At the appliance level, the dissatisfaction coefficients used in the EU reward model are specified per device type. We associate each appliance with a normal distribution and sample heterogeneous dissatisfaction coefficients across households during training [11]. The corresponding mean and standard deviation values for each appliance type are reported in Table 5 and are kept fixed across all experiments.

Table 5: Household appliances and their dissatisfaction parameters (TS: time-shiftable, PC: power-controllable, NI: non-interruptible, I: interruptible).

Appliance	Type	Dissatisfaction coeff.	
		mean	std
Dryer (DR)	TS, NI	0.10	0.10
Washing Machine (WM)	TS, NI	0.40	0.10
Dish Washer (DW)	TS, NI	0.20	0.10
Electric Vehicle (EV)	TS, I	0.05	0.10
Air Conditioner (AC)	PC	3.50	2.00

The DDQN agent uses fully connected policy and target networks with two hidden layers of 128 and 64 ReLU units. Each training episode corresponds to one full day with $H = 24$ hourly time steps, and the agent is trained for $N_{\text{ep}} = 2500$ episodes. At the beginning of each episode, one training day from 2018 is sampled uniformly at random and the corresponding forecasted load and price trajectories are used as the environment input. The policy network is optimised with the Adam algorithm with learning rate $\alpha = 10^{-4}$ and discount factor $\gamma = 0.99$, using a replay buffer of size 50,000 and mini-batches of 256 transitions. We adopt an ε -greedy exploration strategy with $\varepsilon_{\text{start}} = 1.0$, $\varepsilon_{\text{min}} = 0.01$, and exponential decay rate 0.998. The target network parameters are updated using the soft-update rule in Eq.(15) with $\tau = 0.003$.

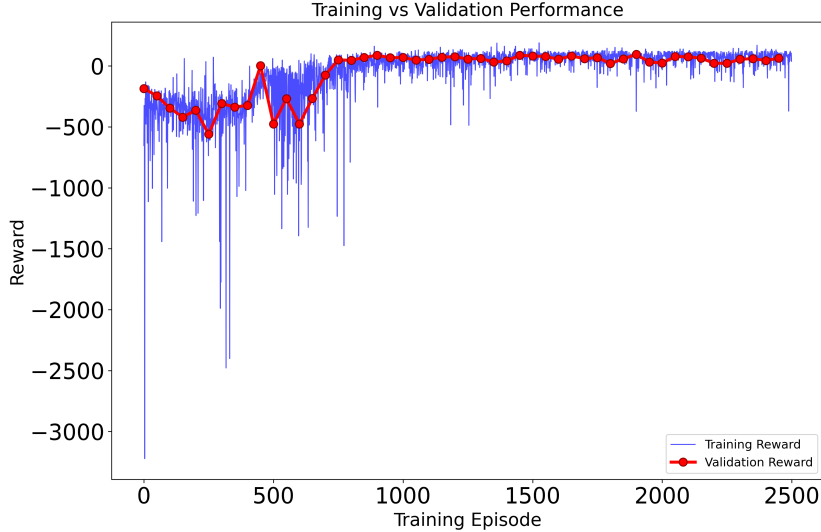


Figure 5: Training and validation episode rewards of the DDQN agent over $N_{\text{ep}} = 2500$ episodes.

The evolution of the DDQN agent’s return during training is illustrated in Fig. 5. The blue curve shows the episode reward on the training set across all $N_{\text{ep}} = 2500$ episodes, whereas the red markers show the average evaluation reward over a small number of validation episodes at regular intervals. At the beginning of learning, the training rewards are strongly negative and exhibit large oscillations, but after a few hundred episodes they gradually increase and, around episodes 800–1000, enter a relatively stable region close to or above zero. The validation rewards follow a similar trend, after an initial transient phase, they fluctuate around a positive and approximately constant level. This behaviour indicates that, under the chosen hyper parameters, the DDQN agent converges to a reasonably stable incentive policy on both the training and validation sets, with no clear evidence of severe overfitting. The remaining variability is mainly due to the stochastic nature of the environment and the use of an ε -greedy exploration policy during training.

5.2.2. Load Reduction and Optimal Incentive Rate

In this part, we examine how the three residential EUs respond to the incentive signals on a representative test day. Fig. 6 shows the energy profile of each EU separately. In each subfigure, the yellow area labelled ‘Demand’ represents the preferred demand profile, whereas the grey hatched area la-

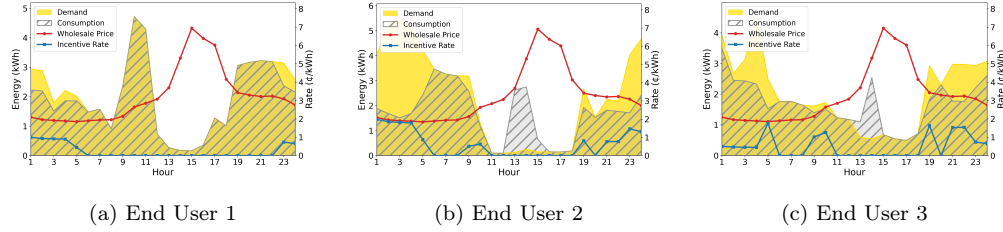


Figure 6: Results of different end users for July 27, 2018.

belled “Consumption” shows the actual consumption after applying the DR scheme.

The RL agent primarily activates incentives during high-load hours when the aggregate demand approaches the capacity threshold. For some households, a portion of the demand is shifted from congested periods to other hours of the same day with lower load. This smooths the individual consumption profile and increases the margin to the aggregate capacity limit. For EUs with larger dissatisfaction coefficients or a higher share of inflexible appliances, the incentive levels remain lower and the achievable reduction is more limited. As a result, their post-DR consumption remains closer to the original pattern. This heterogeneous behaviour shows that the DDQN agent can tailor the incentive rates to the characteristics of each household, including dissatisfaction parameters and the appliance set. The required demand reduction is therefore achieved without imposing excessive discomfort on the participants.

Next, we analyse the aggregate effect of the proposed DR scheme on the aggregated load of the three households and the way the RL agent sets the incentives for the same representative test day. Fig. 7 shows the aggregate load profile of the three households before and after DR together with the capacity threshold. The green dashed line indicates the fixed capacity threshold of 7 kW, which is treated as the maximum allowable aggregate load for these three households.

As can be seen, at the beginning of the day and especially in the evening and night hours, the aggregate load without DR exceeds the 7 kW capacity limit several times. After applying the DR scheme, the main peaks are significantly reduced, and the load profile remains close to, and mostly below the threshold. Part of this difference is due to direct consumption curtailment in congested hours, and part is the result of shifting the demand of flexi-

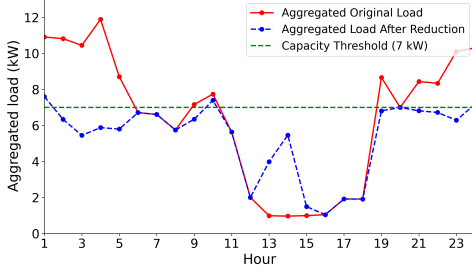


Figure 7: Aggregated load curve with capacity threshold for July 27, 2018.

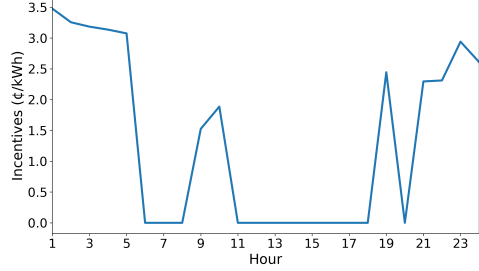


Figure 8: Total hourly incentive rate sent to the three end users on July 27, 2018.

ble appliances from these congested periods to other hours of the same day where the underlying load is lower. Unlike the MARL-iDR profile reported in [11], the CCRL-DR trajectory in Fig. 7 does not exhibit a significant rebound peak after the main peak period. In this way, both the height of the peaks is reduced and the aggregate load profile becomes smoother, without unnecessarily decreasing the total daily energy consumption across all hours.

Fig. 8 shows the total hourly incentives sent to the three households on the same day. The horizontal axis represents the hour of day and the vertical axis the aggregate incentive rate (¢/kWh). Comparing the two figures suggests that the DDQN agent has implicitly learned to account for the capacity limit on the aggregated load and to offer incentives only when they help relieve congestion through load reduction or shifting. Taken together, these two plots summarise the overall behaviour of the proposed DR system.

Table 6 summarises the impact of the proposed CCRL-DR scheme when the results are averaged over all days in July. The peak of the aggregated load is reduced from 11.89 kW under the No-DR to 7.60 kW with CCRL-DR, corresponding to a peak reduction of approximately 36%. The mean load decreases from 6.46 kW to 5.34 kW by about 17%. This suggests that the DR strategy mainly shifts flexible demand to other hours, with only limited direct curtailment, rather than reducing demand uniformly across the day. As a result, the PAR improves from 1.84 to 1.42, corresponding to a reduction of roughly 23%, indicating a flatter daily load profile under the CCRL-DR scheme.

Table 6: Results averaged per day in July

Metric	No DR	CCRL-DR
Peak load (kW)	11.89	7.60
Mean load (kW)	6.46	5.34
PAR	1.84	1.42

5.2.3. Impact of the weighting factor ρ on the financial analysis of the SP and EUs

Table 7 provides a compact summary of the overall financial behaviour of the system when ρ in the EU objective function is varied. For each value of ρ , the table reports, for each EU, the total energy reduction, incentive income, dissatisfaction cost, and net profit. For small values of ρ (e.g., $\rho = 0.1$ and $\rho = 0.3$), the table shows that, for some EUs, the dissatisfaction cost is much larger than the incentive income. As a result, their net profits become negative and the sum of the three EUs' profits is also negative. Under this operating condition, the programme is not economically attractive for the EUs. Table 7 shows that higher values of ρ lead to greater incentive income and lower dissatisfaction costs, and beyond a certain range all three EUs achieve a positive net profit. Under these conditions, the DR programme becomes both technically feasible and financially beneficial for the users.

The lower part of Table 7 characterises the financial performance of the SP. For small values of ρ , the SP profit is high because the revenue from load reduction is large while incentive payments remain relatively small. Under this operating condition, the EUs experience negative net profit. As ρ increases, the DR cost for the SP grows and its profit decreases to some extent, but, in return, the EUs' net profits become positive and their aggregate profit increases. Overall, Table 7 shows that ρ acts as a policy tuning parameter that controls the balance between the SP's benefit and the aggregate benefit of the EUs. For small values of ρ , the system prioritises maximising SP profit at the expense of EU welfare. For larger values of ρ , the SP remains profitable, while a larger share of the DR surplus is transferred to the EUs through incentives, resulting in positive net profit for all parties. This result shows that the choice of ρ should reflect the design objective, whether prioritising SP profit or achieving a more balanced outcome between the SP and the EUs.

Table 7: Financial analyses of the service provider and three end users

Metric	$\rho = 0.1$			$\rho = 0.3$			$\rho = 0.5$			$\rho = 0.7$			$\rho = 0.9$		
	EU1	EU2	EU3	EU1	EU2	EU3	EU1	EU2	EU3	EU1	EU2	EU3	EU1	EU2	EU3
Total energy reduction (kWh)	5.81	14.21	8.7	11.59	17.29	4.99	11.21	17.71	7.26	4.40	6.90	11.08	3.38	21.86	9.66
EU incentive income (€)	0.47	0.77	0.72	5.64	4.3	1.37	8.59	7.77	2.15	5.64	4.82	9.49	2.54	30.58	9.14
EU discomfort cost (€)	2.14	91.81	22.37	6.63	72.90	16.35	4.39	52.83	11.92	1.19	0.87	8.31	0.14	10.83	2.65
EU profit (€)	-1.67	-91.04	-21.65	-0.99	-68.8	-14.97	4.20	-45.05	-9.76	4.45	3.95	1.18	2.40	19.74	6.48
Sum of EU profit (€)		-114.36			-84.56			-50.61			9.58			28.62	
SP gross income of DR (€)		69.34			79.50			92.14			55.57			81.90	
SP Cost of DR (€)		1.97			11.32			18.53			19.96			42.27	
SP profit (€)		67.37			68.17			73.61			35.61			39.62	

To better illustrate the sensitivity of financial outcomes to the weighting factor ρ , Fig. 9 visualizes the variation of the SP profit and the aggregated EU profit reported in Table 7.

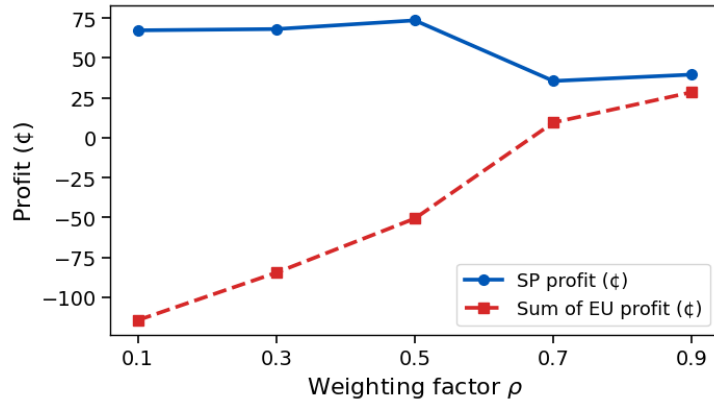


Figure 9: Sensitivity of the service provider profit and the aggregated end-users profit with respect to the weighting factor ρ .

5.2.4. Comparative evaluation with an EBLR approach

In this subsection, we compare the results of the proposed CCRL-DR method with an EBLR approach commonly used in the literature [39, 40, 41, 55]. In this EBLR formulation, the hourly load reduction $\Delta E_{n,h}$ is expressed in Eq. (16). This equation models the reduction as a function of the demand elasticity ξ_h at hour h and the position of the applied incentive rate within its allowable range. Overall, when the incentive is closer to its maximum bound, the expected reduction increases proportionally, while the elasticity coefficient determines the sensitivity of the demand to those incentive changes. The representative values of ξ_h used for different periods of the day are summarised in Table 8.

Table 8: Elasticity in different hours

	Off-peak (1–6 am, 22–24 pm)	Mid-peak (7–16 pm)	On-peak (17–21 pm)
Elasticity ξ_h	0.5	0.3	0.1

Table 9: Three end users' related parameters

EU	μ_n	ω_n	K_{\min}	K_{\max}	λ_{\min}	λ_{\max}
EU1	0.3	0.1	0	$0.3E_{n,h}$	$0.3p_{\min}$	p_{\min}
EU2	0.6					
EU3	0.9					

Two key differences distinguish our CCRL-DR implementation from the EBLR approach. First, in CCRL-DR the load reductions $\Delta E_{n,h}$ are obtained through a device-level HEMS optimisation, whereas in EBLR, $\Delta E_{n,h}$ is computed directly from an aggregate elasticity model in Eq. (16). Consequently, CCRL-DR captures appliance-level flexibility, while EBLR represents EU response only at an aggregate level. Second, CCRL-DR explicitly accounts for the grid capacity limit in both the state and reward formulation, which guides the DDQN agent to concentrate incentives during hours when the aggregated load approaches the capacity threshold. In contrast, the EBLR approach does not incorporate an explicit capacity constraint, and the resulting incentive–response mechanism does not explicitly adapt to actual network congestion conditions.

To enable a meaningful comparison, the EBLR approach is applied to the same three households and uses the same forecasted price and load trajectories, and time horizon as in the CCRL-DR experiments. The elasticity coefficients ξ_h (Table 8) and the EU-related parameters μ_n , ω_n , K_{\min} , K_{\max} , λ_{\min} and λ_{\max} (Table 9) are loosely adapted from the illustrative settings in [39] and have been adjusted to match the characteristics of our three-household case study. These parameters are used only within the EBLR formulation.

$$\Delta E_{n,h} = E_{n,h} \cdot \xi_h \cdot \frac{\lambda_{n,h} - \lambda_{\min}}{\lambda_{\min}} \quad (16)$$

Fig. 10 compares the hourly demand profiles of the three residential EUs on

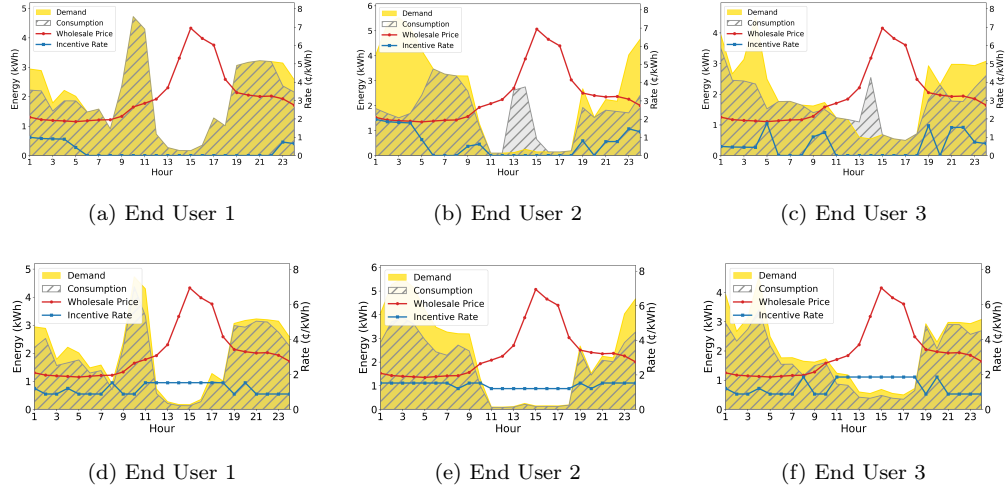


Figure 10: Comparison of energy profiles for three residential end users under the CCRL-DR (top row) and EBLR (bottom row) approaches on July 27, 2018.

the selected summer day. In the CCRL-DR case (top row), household demand is adjusted through appliance-level responses to the incentive signals. This results in targeted peak shaving through both load curtailment and time shifting at the household level. Consequently, reductions are concentrated around local peak hours, while non-critical periods are only marginally affected. In contrast, the EBLR profiles (bottom row) are obtained from an elasticity-based EU-level response, without explicitly enforcing the network capacity constraint. As a result, the post-DR profiles exhibit more diffuse and proportional reductions, without the same degree of structure around the critical hours. Peak consumption is lowered to some extent, but the pattern of curtailment is less tightly aligned with the network congestion periods. Overall, Fig. 10 shows that CCRL-DR exploits household heterogeneity more effectively, producing targeted demand adjustments around critical hours, whereas EBLR leads to a more uniform elastic response.

Fig. 11 moves from the household perspective to the system perspective by plotting the aggregated load of the three EUs. In the CCRL-DR case, the aggregated load is explicitly constrained by the capacity limit. This leads to a clear alignment between the incentive pattern and the periods when the aggregated load is close to the capacity limit. The aggregated post-DR curve is consistently kept at or below the capacity threshold during the critical hours, while it closely follows the original profile in non-congested periods.

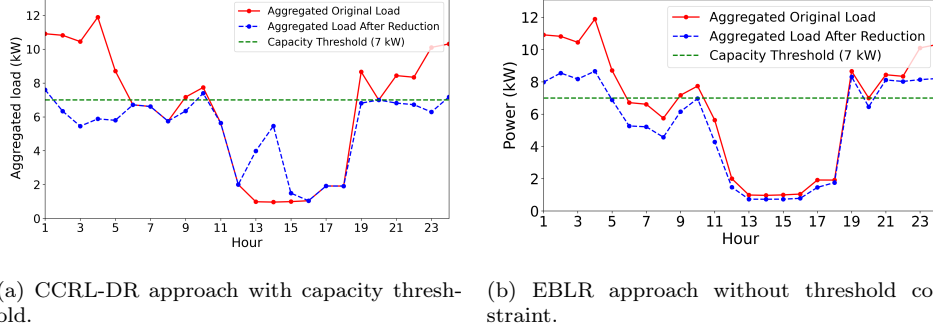


Figure 11: Comparison of aggregated load curves for July 27, 2018 under the CCRL-DR (left) and EBLR (right) methods. The figure illustrates differences in peak load behaviour between the two approaches.

In other words, CCRL-DR concentrates flexibility in the most critical periods without unnecessarily reducing demand elsewhere. In the EBLR case, aggregate reductions are driven by elasticity-based responses without explicit consideration of network constraints. Although the overall load is reduced, the timing and magnitude of the reductions are driven mainly by the elasticity parameters rather than by network conditions. As a consequence, the post-DR aggregate profile under EBLR can still approach or exceed the capacity limit during peak hours, while part of the reduction occurs in less critical periods. Fig. 11 thus highlights the main system-level advantage of CCRL-DR; by embedding the capacity limit directly into the RL state and reward, it produces DR actions that are explicitly aware of this constraint, whereas the elasticity-based benchmark does not enforce it.

Fig. 12 compares three key indicators of the aggregated load profile under three operating modes: No DR, the benchmark EBLR, and the proposed CCRL-DR. The bars show the daily peak demand, the daily mean demand, and the PAR for each case. Both DR schemes reduce the peak demand relative to the No DR, but CCRL-DR achieves the largest reduction, consistent with the behaviour observed in the aggregated load profiles. At the same time, the mean demand under CCRL-DR is only moderately lower than in the No DR, indicating that the scheme focuses on the most critical hours rather than uniformly reducing consumption across the whole day. As a result, CCRL-DR achieves the lowest PAR among the three cases, reflecting a flatter load profile that better respects the capacity limit. Overall, Fig. 12 shows that CCRL-DR achieves a more effective balance between peak reduc-

tion and energy conservation.

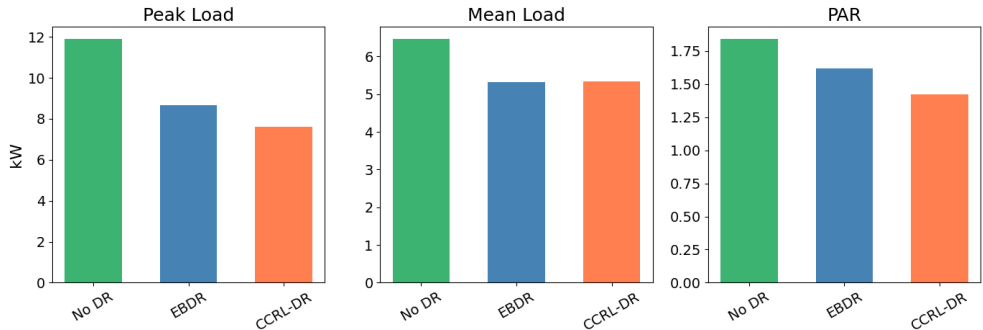


Figure 12: Comparison of average peak load, mean load, and PAR for No DR, EBLR, and CCRL-DR approaches on July 27, 2018.

6. Conclusion and future work

This paper presented a capacity-constrained incentive-based demand response framework for residential smart grids, in which an SP employs a DRL approach to determine real-time incentive rates under explicit grid capacity limits. Heterogeneous EU preferences were modelled through appliance-level HEMMs and dissatisfaction costs, enabling differentiated and adaptive incentive design. In the considered case study, the aggregated load remains close to the capacity threshold without inducing rebound peaks, resulting in a 22.82% reduction in the PAR compared to the no-DR case. These results highlight the potential of combining capacity-aware incentive learning with appliance-level flexibility to improve grid performance while maintaining EU comfort.

Future work will extend the proposed single-agent RL framework by incorporating cluster formation techniques to improve scalability and coordination across larger populations of EUs. By grouping households with similar consumption patterns or flexibility characteristics, the SP will be able to design cluster-level incentive policies while preserving appliance-level comfort modelling. This extension is expected to reduce the dimensionality of the decision space and enhance learning efficiency, while maintaining user comfort and effective capacity-aware demand response performance.

Data and Code Availability Statement

We used publicly available datasets in this study. Residential electricity consumption data were obtained from Pecan Street Inc., Dataport, available at: <https://dataport.pecanstreet.org/>, and wholesale electricity price data were obtained from EnergyOnline, available at: <https://www.energyonline.com/>. To support reproducibility, the complete implementation and data preparation instructions are available in our GitHub repository: GitHub repository

References

- [1] F. Alfaverh, M. Denai, Y. Sun, Demand response strategy based on reinforcement learning and fuzzy reasoning for home energy management, *IEEE access* 8 (2020) 39310–39321.
- [2] U.S. Department of Energy, Benefits of demand response in electricity markets and recommendations for achieving them, Tech. rep., U.S. Department of Energy, Washington, DC, USA (2006).
- [3] M. Yu, S. H. Hong, Supply–demand balancing for power management in smart grid: A stackelberg game approach, *Applied energy* 164 (2016) 702–710.
- [4] A. Shewale, A. Mokhade, N. Funde, N. D. Bokde, An overview of demand response in smart grid and optimization techniques for efficient residential appliance scheduling problem, *Energies* 13 (16) (2020) 4266.
- [5] B. Parrish, P. Heptonstall, R. Gross, B. K. Sovacool, A systematic review of motivations, enablers and barriers for consumer engagement with residential demand response, *Energy Policy* 138 (2020) 111221.
- [6] B. Parrish, R. Gross, P. Heptonstall, On demand: Can demand response live up to expectations in managing electricity systems?, *Energy Research & Social Science* 51 (2019) 107–118.
- [7] S. Oh, J. Kong, Y. Yang, J. Jung, C.-H. Lee, A multi-use framework of energy storage systems using reinforcement learning for both price-based and incentive-based demand response programs, *International Journal of Electrical Power & Energy Systems* 144 (2023) 108519.

- [8] B. Shen, G. Ghatikar, Z. Lei, J. Li, G. Wikler, P. Martin, The role of regulatory reforms, market changes, and technology development to make demand response a viable resource in meeting energy challenges, *Applied Energy* 130 (2014) 814–823.
- [9] X. Yan, Y. Ozturk, Z. Hu, Y. Song, A review on price-driven residential demand response, *Renewable and Sustainable Energy Reviews* 96 (2018) 411–419.
- [10] A. Ghasemkhani, L. Yang, J. Zhang, Learning-based demand response for privacy-preserving users, *IEEE Transactions on Industrial Informatics* 15 (9) (2019) 4988–4998.
- [11] J. van Tilburg, L. C. Siebert, J. L. Cremer, Marl-idr: Multi-agent reinforcement learning for incentive-based residential demand response, in: 2023 IEEE Belgrade PowerTech, IEEE, 2023, pp. 1–8.
- [12] M. Eissa, First time real time incentive demand response program in smart grid with “i-energy” management system with different resources, *Applied energy* 212 (2018) 607–621.
- [13] Y.-C. Li, S. H. Hong, Real-time demand bidding for energy management in discrete manufacturing facilities, *IEEE Transactions on Industrial Electronics* 64 (1) (2016) 739–749.
- [14] A. Asadinejad, K. Tomsovic, Optimal use of incentive and price based demand response to reduce costs and price volatility, *Electric Power Systems Research* 144 (2017) 215–223.
- [15] N. Eslaminia, H. R. Mashhadi, Enhancing peak shaving through non-linear incentive-based demand response: A consumer-centric utility optimization approach, *International Transactions on Electrical Energy Systems* 2023 (1) (2023) 4650539.
- [16] M. S. Bakare, A. Abdulkarim, M. Zeeshan, A. N. Shuaibu, A comprehensive overview on demand side energy management towards smart grids: challenges, solutions, and future direction, *Energy Informatics* 6 (1) (2023) 4.

- [17] F. Pallonetto, M. De Rosa, F. D’Ettorre, D. P. Finn, On the assessment and control optimisation of demand response programs in residential buildings, *Renewable and Sustainable Energy Reviews* 127 (2020) 109861.
- [18] S. Panda, S. Mohanty, P. K. Rout, B. K. Sahu, M. Bajaj, H. M. Zawbaa, S. Kamel, Residential demand side management model, optimization and future perspective: A review, *Energy Reports* 8 (2022) 3727–3766.
- [19] X. Fang, Q. Hu, F. Li, B. Wang, Y. Li, Coupon-based demand response considering wind power uncertainty: A strategic bidding model for load serving entities, *IEEE Transactions on Power Systems* 31 (2) (2015) 1025–1037.
- [20] Z. Li, S. Wang, X. Zheng, F. De Leon, T. Hong, Dynamic demand response using customer coupons considering multiple load aggregators to simultaneously achieve efficiency and fairness, *IEEE Transactions on Smart Grid* 9 (4) (2016) 3112–3121.
- [21] O. Erdinc, A. Taşcikaraoglu, N. G. Paterakis, J. P. Catalao, Novel incentive mechanism for end-users enrolled in dlc-based demand response programs within stochastic planning context, *IEEE Transactions on Industrial Electronics* 66 (2) (2018) 1476–1487.
- [22] M. Yu, S. H. Hong, Incentive-based demand response considering hierarchical electricity market: A stackelberg game approach, *Applied Energy* 203 (2017) 267–279.
- [23] M. Yu, S. H. Hong, Y. Ding, X. Ye, An incentive-based demand response (dr) model considering composited dr resources, *IEEE Transactions on Industrial Electronics* 66 (2) (2018) 1488–1498.
- [24] E. Shahryari, H. Shayeghi, B. Mohammadi-Ivatloo, M. Moradzadeh, An improved incentive-based demand response program in day-ahead and intra-day electricity markets, *Energy* 155 (2018) 205–214.
- [25] A. Asadinejad, A. Rahimpour, K. Tomsovic, H. Qi, C.-f. Chen, Evaluation of residential customer elasticity for incentive based demand response programs, *Electric Power Systems Research* 158 (2018) 26–36.

- [26] M. A. F. Ghazvini, P. Faria, S. Ramos, H. Morais, Z. Vale, Incentive-based demand response programs designed by asset-light retail electricity providers for the day-ahead market, *Energy* 82 (2015) 786–799.
- [27] M. A. F. Ghazvini, J. Soares, N. Horta, R. Neves, R. Castro, Z. Vale, A multi-objective model for scheduling of short-term incentive-based demand response programs offered by electricity retailers, *Applied energy* 151 (2015) 102–118.
- [28] J. Vuelvas, F. Ruiz, G. Gruosso, Limiting gaming opportunities on incentive-based demand response programs, *Applied Energy* 225 (2018) 668–681.
- [29] M. Rahmani-Andebili, Modeling nonlinear incentive-based and price-based demand response programs and implementing on real power markets, *Electric Power Systems Research* 132 (2016) 115–124.
- [30] M. Rahmani-Andebili, Nonlinear demand response programs for residential customers with nonlinear behavioral models, *Energy and Buildings* 119 (2016) 352–362.
- [31] J. R. Vázquez-Canteli, Z. Nagy, Reinforcement learning for demand response: A review of algorithms and modeling techniques, *Applied energy* 235 (2019) 1072–1089.
- [32] E. J. Salazar, M. Jurado, M. E. Samper, Reinforcement learning-based pricing and incentive strategy for demand response in smart grids, *Energies* 16 (3) (2023) 1466.
- [33] G. T. Costanzo, S. Iacovella, F. Ruelens, T. Leurs, B. J. Claessens, Experimental analysis of data-driven control for a building heating system, *Sustainable Energy, Grids and Networks* 6 (2016) 81–90.
- [34] C. Mahapatra, A. K. Moharana, V. C. Leung, Energy management in smart cities based on internet of things: Peak demand reduction and energy savings, *Sensors* 17 (12) (2017) 2812.
- [35] V. Kansal, A.-A. Kassem, R. Kumar, N. S. Boob, S. Anand, P. Gupta, Optimizing energy consumption in smart buildings through reinforcement learning-based demand response strategies, in: 2024 International

Conference on Communication, Computer Sciences and Engineering (IC3SE), IEEE, 2024, pp. 1616–1621.

- [36] K. Ren, J. Liu, Z. Wu, X. Liu, Y. Nie, H. Xu, A data-driven drl-based home energy management system optimization framework considering uncertain household parameters, *Applied Energy* 355 (2024) 122258.
- [37] X. Xu, Y. Jia, Y. Xu, Z. Xu, S. Chai, C. S. Lai, A multi-agent reinforcement learning-based data-driven method for home energy management, *IEEE Transactions on Smart Grid* 11 (4) (2020) 3201–3211.
- [38] I. Dusparic, A. Taylor, A. Marinescu, V. Cahill, S. Clarke, Maximizing renewable energy use with decentralized residential demand response, in: 2015 IEEE first international smart cities conference (ISC2), IEEE, 2015, pp. 1–6.
- [39] R. Lu, S. H. Hong, Incentive-based demand response for smart grid with reinforcement learning and deep neural network, *Applied energy* 236 (2019) 937–949.
- [40] L. Wen, K. Zhou, J. Li, S. Wang, Modified deep learning and reinforcement learning for an incentive-based demand response model, *Energy* 205 (2020) 118019.
- [41] H. Xu, W. Kuang, J. Lu, Q. Hu, A modified incentive-based demand response model using deep reinforcement learning, in: 2020 12th IEEE PES Asia-Pacific Power and Energy Engineering Conference (APPEEC), IEEE, 2020, pp. 1–5.
- [42] H.-M. Chung, S. Maharjan, Y. Zhang, F. Eliassen, Distributed deep reinforcement learning for intelligent load scheduling in residential smart grids, *IEEE Transactions on Industrial Informatics* 17 (4) (2020) 2752–2763.
- [43] C. Zhang, S. R. Kuppannagari, C. Xiong, R. Kannan, V. K. Prasanna, A cooperative multi-agent deep reinforcement learning framework for real-time residential load scheduling, in: Proceedings of the international conference on internet of things design and implementation, 2019, pp. 59–69.

- [44] R. Lu, S. H. Hong, M. Yu, Demand response for home energy management using reinforcement learning and artificial neural network, *IEEE Transactions on Smart Grid* 10 (6) (2019) 6629–6639.
- [45] M. Fahrioglu, F. L. Alvarado, Using utility information to calibrate customer demand management behavior models, *IEEE transactions on power systems* 16 (2) (2002) 317–322.
- [46] V. Mnih, K. Kavukcuoglu, D. Silver, A. A. Rusu, J. Veness, M. G. Bellemare, A. Graves, M. Riedmiller, A. K. Fidjeland, G. Ostrovski, et al., Human-level control through deep reinforcement learning, *nature* 518 (7540) (2015) 529–533.
- [47] L. Xi, L. Yu, Y. Xu, S. Wang, X. Chen, A novel multi-agent ddqn-ad method-based distributed strategy for automatic generation control of integrated energy systems, *IEEE Transactions on Sustainable Energy* 11 (4) (2019) 2417–2426.
- [48] H. Van Hasselt, A. Guez, D. Silver, Deep reinforcement learning with double q-learning, in: *Proceedings of the AAAI Conference on Artificial Intelligence*, Vol. 30, 2016, pp. 2094–2100.
- [49] A. G. Barto, Reinforcement learning: An introduction. by richard's sutton, *SIAM Rev* 6 (2) (2021) 423.
- [50] Pecan Street Inc., Dataport, <https://dataport.cloud/>, accessed: July 14, 2025 (2025).
- [51] EnergyOnline, EnergyOnline: Electricity Market and Energy Industry News, <https://www.energyonline.com/>, accessed: July 14, 2025 (2025).
- [52] K. Choi, J. Yi, C. Park, S. Yoon, Deep learning for anomaly detection in time-series data: Review, analysis, and guidelines, *IEEE access* 9 (2021) 120043–120065.
- [53] M. Abumohsen, A. Y. Owda, M. Owda, Electrical load forecasting using lstm, gru, and rnn algorithms, *Energies* 16 (5) (2023) 2283.
- [54] G. Memarzadeh, F. Keynia, Short-term electricity load and price forecasting by a new optimal lstm-nn based prediction algorithm, *Electric Power Systems Research* 192 (2021) 106995.

[55] R. Lu, S. H. Hong, X. Zhang, A dynamic pricing demand response algorithm for smart grid: Reinforcement learning approach, *Applied energy* 220 (2018) 220–230.